THE JOURNAL OF BIOLOGICAL CHEMISTRY VOL. 281, NO. 27, pp. 18753–18762, July 7, 2006

PACSINs Bind to the TRPV4 Cation Channel

*PACSIN 3 MODULATES THE SUBCELLULAR LOCALIZATION OF TRPV4**

Received for publication, March 15, 2006, and in revised form, April 17, 2006 Published, JBC Papers in Press, April 20, 2006, DOI 10.1074/jbc.M602452200

Math P. Cuajungco[‡1], Christian Grimm[‡1], Kazuo Oshima[‡], Dieter D'hoedt[§], Bernd Nilius[§], Arjen R. Mensenkamp[¶], René J. M. Bindels[¶], Markus Plomann[‖], and Stefan Heller[‡2]

From the [‡]Departments of Otolaryngology, Head and Neck Surgery and Molecular & Cellular Physiology, Stanford University School of Medicine, Stanford California 94305, [§]Department of Physiology, Campus Gasthuisberg, Katholieke Universiteit Leuven, 3000 Leuven, Belgium, the [¶]Department of Physiology, Radboud University Nijmegen, 6500 Nijmegen, The Netherlands, and the [‖]Cellular Neurobiology Unit, Center for Biochemistry and Center for Molecular Medicine, University of Cologne, D-50931 Cologne, Germany

TRPV4 is a cation channel that responds to a variety of stimuli including mechanical forces, temperature, and ligand binding. We set out to identify TRPV4-interacting proteins by performing yeast two-hybrid screens, and we isolated with the avian TRPV4 amino terminus the chicken orthologues of mammalian PACSINs 1 and 3. The PACSINs are a protein family consisting of three members that have been implicated in synaptic vesicular membrane trafficking and regulation of dynamin-mediated endocytotic processes. In biochemical interaction assays we found that all three murine PACSIN isoforms can bind to the amino terminus of rodent TRPV4. No member of the PACSIN protein family was able to biochemically interact with TRPV1 and TRPV2. Co-expression of PACSIN 3, but not PACSINs 1 and 2, shifted the ratio of plasma membrane-associated *versus* cytosolic TRPV4 toward an apparent increase of plasma membrane-associated TRPV4 protein. A similar shift was also observable when we blocked dynamin-mediated endocytotic processes, suggesting that PACSIN 3 specifically affects the endocytosis of TRPV4, thereby modulating the subcellular localization of the ion channel. Mutational analysis shows that the interaction of the two proteins requires both a TRPV4-specific proline-rich domain upstream of the ankyrin repeats of the channel and the carboxyl-terminal Src homology 3 domain of PACSIN 3. Such a functional interaction could be important in cell types that show distribution of both proteins to the same subcellular regions such as renal tubule cells where the proteins are associated with the luminal plasma membrane.

The TRPV4 protein, initially described as OTRPC4 (1), VR-OAC (2), TRP12 (3), and VRL-2 (4), is a member of the TRPV (vanilloid-type transient receptor potential) superfamily consisting of mainly nonspecific cation channels. Like many other transient receptor potential ion channels, TRPV4 contains three ankyrin-like repeat domains in its amino-terminal intracellular domain, six putative transmembrane-spanning domains, a pore loop region, and a transient receptor potential domain near its carboxyl terminus. TRPV4 is activated by exposure to hypotonicity (1, 2), although it has recently been proposed that this activation is mediated by second messengers (5, 6). Osmosensation is a form of mechanosensation mediated by ion channels or associated structures that measure tension in membranes or in other elastic elements. In agreement with its proposed function in osmosensation, TRPV4 mRNA transcript is found in epithelial cells of kidney tubules, in the *stria vascularis* of the cochlea, in sweat glands, and in the osmosensory cells of the circumventricular organs of the brain (1, 2). Interestingly, the distribution of TRPV4 protein in other tissues such as airway smooth muscle, oviduct, spleen, heart, liver, testis, keratinocyte, inner ear hair cells, and dorsal root ganglion suggests that the role of this channel is not at all restricted to osmosensation. This notion is supported by reports of a variety of other stimuli that activate TRPV4. For example, increasing the temperature above 27 °C has been found to activate TRPV4 (2, 7, 8). Likewise, TRPV4 is gated by synthetic agonists such as the phorbol ester 4-α-phorbol-12,13-didecanoate (8, 9) and endogenous agonist precursors such as the endocannabinoid anandamide, or its hydrolysis product, arachidonic acid, which is metabolized into 5′,6′-epoxyeicosatrienoic acid by cytochrome P-450 epoxygenase (5). Particularly, the 5′,6′-epoxyeicosatrienoic acid metabolite is a potent activator of TRPV4 (5, 10).

The involvement of TRPV4 in sensing a variety of stimuli *in vivo* was shown by recent studies demonstrating: (i) that TRPV4 is necessary for a circumventricular organ-mediated osmosensation in the CNS (11); (ii) that thermosensation and nociception is mediated by TRPV4 in mouse skin keratinocytes (12) and human mammary keratinocytes (13), respectively; (iii) that TRPV4 functions as osmotically gated transducer in primary afferent nociceptive nerve fibers (12, 14); and (iv) that nociception through TRPV4 may well be transduced through a mechanosensory process (15–17).

It has been hypothesized that the mechanical/osmotic gating of TRPV4 by cell swelling is dependent on active phospholipase A_2, an enzyme necessary for arachidonic acid synthesis (5, 10). A second messenger-based activation of TRPV4 is consistent with previous electrophysiological findings showing that, by switching from a cell-attached to a cell-detached patch clamp modus, the open probability of TRPV4 substantially decreases (2). This phenomenon could also be interpreted as a direct result of the essential requirement of the ion channel for a specific association with intracellular structures. Notwithstanding such penumbral structure-function relation of the TRPV4 gating mechanisms, we hypothesized that TRPV4 interacts with other proteins and that such association may determine the subcellular targeting of TRPV4, its retention in distinct membrane regions, or its withdrawal from the plasma membrane. As a first step toward the identification of interaction partners, we conducted a yeast two-hybrid screen for

* This work was supported by National Institutes of Health Grant DC04563 (to S. H.), by Human Frontier Science Program Research Grant RPG0032/2004 (to R. J. M. B., B. N., and S. H.), and by Deutsche Forschungsgemeinschaft Grant PL 233/3-1 (to M. P.). The costs of publication of this article were defrayed in part by the payment of page charges. This article must therefore be hereby marked "*advertisement*" in accordance with 18 U.S.C. Section 1734 solely to indicate this fact.

[1] These authors contributed equally to this work.

[2] To whom correspondence should be addressed: Depts. of Otolaryngology and Molecular & Cellular Physiology, Stanford University School of Medicine, 801 Welch Rd., Stanford, CA 94305-5739. Tel.: 650-725-6500; Fax: 650-725-8502; E-mail: hellers@stanford.edu.

TRPV4-binding proteins, and we identified the PACSINs, a group of three proteins, each encoded by an individual gene, as TRPV4-binding partners. We provide evidence that this interaction happens between the carboxyl-terminal SH3[3] domain that is present in all three PACSINs and a triple-proline motif within the amino-terminal proline-rich domain (PRD) of TRPV4. Recent studies suggest that PACSIN proteins functionally interact with the endocytotic machinery and participate in synaptic vesicular targeting (18). Here we report that co-expression of PACSIN 3, but not PACSINs 1 and 2, shifts the ratio between intracellular and plasma membrane-associated TRPV4 toward an apparent retention of the protein in or near the plasma membrane.

MATERIALS AND METHODS

Yeast Two-hybrid Screen and Two-hybrid Assays—Two-hybrid bait vectors were generated by PCR from chicken TRPV4 cDNA (accession number NM_204692) (2). We used the following primer pairs: the amino-terminal fragment (amino acids 1–453), forward, 5′-gaGAATTCatggcagaccccgaagacccccgtg-3′, and reverse, 5′-gagaGTCGACagcaccgaacttgcgc-3′; first intracellular loop (amino acids 514–539), forward, 5′-gaGAATTCaatatcaaagatctcttcatg-3′, and reverse, 5′-gagaGTCGACtcagtagaggcagctgaaatgagcc-3′; second intracellular loop (amino acids 577–606), forward, 5′-gaGAATTCtacttcacgcgagggctcaagc-3′, and reverse, 5′-gagaGTCGACtcagaccaggaggaagcggaacag-3′; and carboxyl-terminal fragment (amino acids 699–852), forward, 5′-gaGAATTCatgctcatcgccctcatgggtg-3′, and reverse, 5′-gagaGTCGACctagagtggggagctgggggtc-3′. Restriction enzyme recognition sites for EcoRI and SalI (indicated in uppercase letters in the primer sequences) were used to subclone the amplified cDNA fragments in frame with the Gal4 binding domain into the yeast-*Escherichia coli* shuttle vector pBD-GAL4 Cam (Stratagene). The identities and integrity of the cDNA inserts were confirmed by sequencing. For screening, we first transformed yeast strain AH109 (Clontech) with each of the bait vectors, and then we individually transformed each bait-containing yeast cell population with plasmid DNA prepared from a chicken basilar papilla cDNA library in the HybriZAP two-hybrid bacteriophage λ vector (19). Auto-activation in bait-containing yeast cells was suppressed by adding 5 mM of the competitive His3 protein inhibitor 3-amino-1,2,4-triazole to the dropout medium. For each bait, 2×10^7 transformants were selectively screened for Gal4-induced activation of the *HIS3* and *ADE2* genes by using the lithium acetate/single-stranded carrier DNA/polyethylene glycol method (20). Clones were considered positive when they conferred histidine autotrophy to a deficient yeast strain and when they led to expression of the reporter enzyme β-galactosidase assayed by conversion of colorless 5-bromo-4-chloro-3-indolyl-β-D-galactopyranoside (X-Gal) to a blue precipitate. Only cDNAs that were isolated multiple times independently were further studied. Positive colonies were further tested for expression of the Gal-4-dependent reporter *lacZ* by filter lift assay (for details, see HybriZAP-2.1 two-hybrid cDNA synthesis kit manual (Stratagene) and Matchmaker Gal4 Two-Hybrid System 3 user manual (Clontech)). Library cDNA in pAD-GAL4 phagemid vector was recovered from individual yeast colonies via ampicillin selection, and cDNA inserts were sequence-verified.

Antibodies—To generate antibodies to TRPV4, the amino terminus of rat TRPV4 (amino acids 1–233) lacking the ankyrin repeats was obtained by PCR with a hexahistidine moiety at its carboxyl terminus and subcloned into the pFastBac1 vector (Invitrogen). Recombinant TRPV4 amino terminus was expressed in insect cells (SF9; Invitrogen) and purified under native conditions with Ni^{2+}-conjugated agarose beads (nickel-nitrilotriacetic acid; Qiagen). Two female rabbits were each initially immunized with 200 μg of the recombinant TRPV4 amino terminus; additional boost injections were given at 2–3-week intervals (Covance). The sera of both animals displayed strong reactivity against the immunogen in Western blots. All of the experiments described in this publication were done with the combined final bleed sera of both rabbits and were enriched by affinity purification on a column generated with recombinant TRPV4 amino-terminal protein (Ultralink; Pierce). Antibody specificity was shown by blocking the signal on Western blots via preincubating the anti-TRPV4 polyclonal sera with the amino-terminal TRPV4 polypeptide (Fig. 1*A*). Another control for antibody specificity was demonstrated by comparing Western blots of kidney and keratinocyte protein extracts from *trpv4*-null mice and wild-type littermates (11, 12). We also used previously characterized affinity-purified antibodies to glutathione *S*-transferase fusion proteins of PACSINs 1, 2, and 3 (18, 21, 22).

Polyclonal anti-TRPV1 and anti-TRPV2 antibodies were purchased from Calbiochem EMD Biosciences (San Diego, CA). The manufacturer demonstrates specificity of these antibodies by blocking the signal on Western blots through preincubation of the antibodies with excess antigen (see manufacturer's product description). 9E10 monoclonal antibody to c-Myc was obtained from the Developmental Studies Hybridoma Bank and immobilized on agarose beads from a commercial supplier (ProFound c-Myc-Tag immunoprecipitation kit; Pierce).

Co-immunoprecipitation—For co-immunoprecipitation, we generated expression vectors for the interaction partners using the plasmid pcDNA3.1 (Invitrogen). We also used the TOPO-pCR8/pTREX Gateway vector systems (Invitrogen) to subclone and express the full-length murine cDNAs of TRPV1, TRPV2, and TRPV4 proteins. The corresponding primer pairs to amplify these cDNAs were: (i) TRPV1-forward, 5′-aagcttaccatggagaaatgggctagcttaga-3′, and TRPV1-reverse, 5′-tctagatttatttcattatttctcccctggggccatgga-3′; (ii) TRPV2-forward, 5′-gaattcaccatgacttcagcctccaacccc-3′, and TRPV2-reverse, 5′-ctcgagtttattcattagtgggactggaggacctgaag-3′; and (iii) TRPV4-forward, 5′-aagcttaccatggcagatcctggtgatggtc-3′, and TRPV4-reverse, 5′-tctagatttatttcattacagtggggcatcgtccgtcct-3′. The deletion and point mutations were introduced by PCR, and the resulting amplification products were subcloned into the pCDNA3.1 expression vector and sequence-verified.

The cell lines HEK293, HeLa, and NIH 3T3 were transfected with single plasmids or with combinations of the expression vectors using Lipofectamine 2000 (Invitrogen) or polyethylinimine (Polysciences, Inc.). Transfected cells were washed with cold PBS 48 h after transfection and lysed in ice-cold precipitation assay buffer consisting of 150 mM NaCl, 1% octylphenyl-polyethylene glycol (Igepal CA-630), 0.5% sodium deoxycholate, 0.1% sodium dodecyl sulfate in 50 mM Tris at pH 7.5. For immunoprecipitation, we used immobilized monoclonal anti-c-Myc agarose beads and performed the experiments according to the manufacturer's recommendation. Alternatively, we added 9E10 monoclonal antibody to c-Myc at a dilution of 1:250 to cell lysates. Following 2 h of incubation at 4 °C, immunoglobulins and bound proteins were precipitated from the lysate with protein A-agarose (Affi-Gel; Bio-Rad), washed four times with precipitation assay buffer, and the bound proteins were separated by polyacrylamide gel electrophoresis. All of the immunoprecipitation-bound proteins were subjected to high stringency washes with 500 mM NaCl in Tris-buffered saline plus 1% Tween 20. Each immunoprecipitation was controlled by mock experiments without the addition of antibody. The omission of the antibody and the use of cell lysates from control-transfected cells always confirmed the specificity of the results presented in this study.

[3] The abbreviations used are: SH, Src homology; PRD, proline-rich domain; PBS, phosphate-buffered saline; DIP, dynamin inhibitory peptide; FITC, fluorescein isothiocyanate; 4α-PDD, 4α-phorbol 12,13-dideconate; RT, reverse transcription.

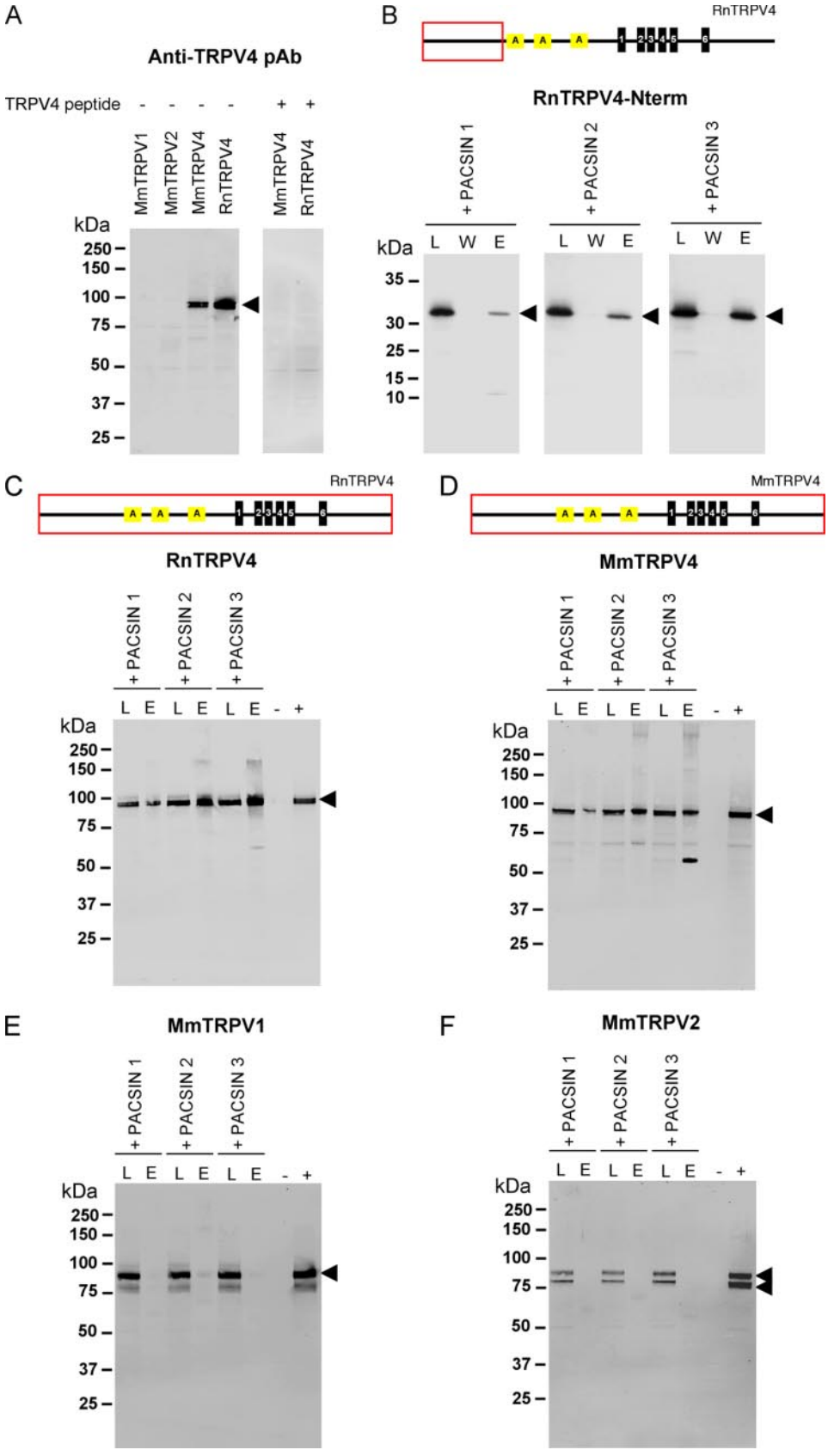

FIGURE 1. **TRPV4 antibody characterization and binding of all three PACSINs to mammalian TRPV4.** *A*, control experiment with lysates from HEK293 cells transfected with expression vectors for murine TRPV1, TRPV2, TRPV4, and rat TRPV4. Note that the specific double band running between 95 and 100 kDa is blocked after preincubation of the TRPV4 antibody with the amino-terminal TRPV4 polypeptide. *B*, analysis of interactions between rat TRPV4 amino terminus (amino acids 1–239, indicated by the *red box* in the schematic drawing) and murine PACSIN proteins. The Myc-tagged PACSINs were precipitated with 9E10 antibody, and the detection was performed with antibody to TRPV4 (*black arrowheads* point to the ~32-kDa TRPV4 amino-terminal fragment). *C–F*, Western blots showing co-immunoprecipitation of full-length rat TRPV4 (*C*) and murine TRPV4 (*D*), but not murine TRPV1 (*E*) and murine TRPV2 (*F*) with PACSINs 1, 2, and 3. Specific bands (*arrowheads*) were detected with antibody to TRPV4, TRPV1, and TRPV2, respectively. Immunoprecipitation was done with immobilized 9E10 antibody. The ~60-kDa band in the *TRPV4:Pacsin 3 E lane* in *D* was observable in some but not all experiments. *L*, lysate; *E*, eluate from immunoprecipitate; −, lysate from untransfected negative control; +, lysate from TRPV4-transfected positive control.

Western Blots and Immunocytochemistry—Western blots were incubated for 1 h at room temperature in 2.5% (v/v) Liquid Block (Amersham Biosciences) and 0.1% (v/v) Tween 20 in PBS (PBS-T). The blots were incubated overnight at 4 °C with antiserum diluted in PBS-T with 2.5% Liquid Block. The following antiserum dilutions were used: 1:5000 for monoclonal 9E10 anti-c-Myc antibody; 1:5000 for rabbit anti-

PACSIN 3; 1:10000 rabbit anti-TRPV4; 1:1000 for rabbit anti-mouse TRPV1; and 1:1000 for rabbit anti-mouse TRPV2. The blots were washed four times for 10 min each at room temperature. Detection was performed with IRDye 700- and IRDye 800-conjugated secondary antibodies (Rockland Immunochemicals, Gilbertsville, PA) and scanning with the Odyssey infrared imaging system (LI-COR Biosciences, Lincoln, NE).

Transfected human cell lines HEK293, HeLa, and mouse NIH 3T3 cells were used for immunofluorescence studies. Kidney tissue was taken from wild-type C57BL/6 mouse (Charles River Labs, MA) and fixed with 4% paraformaldehyde-fixed for cryosections. The cultured cells were fixed with methanol. All of the specimens were blocked in 0.1% Triton-100, 1% bovine serum albumin (w/v), and 5% (w/v) heat-inactivated goat serum in PBS (PBT1). The slides or cells were then incubated overnight at 4 °C using the following antibodies: rabbit anti-TRPV4 (1:500 dilution), rabbit anti-PACSIN 1, 2, or 3 (1:250 dilution), mouse anti-c-Myc (9E10; 1:500), red fluorescent Alexa Fluor 594 wheat germ agglutinin (1:200 dilution, Invitrogen), rabbit anti-mouse TRPV1 (1:250 dilution), and rabbit anti-mouse TRPV2 (1:500). Unbound antibodies were removed by three PBT1 washes and one PBT2 (same formulation as PBT1 but without the serum) wash for 15 min each at room temperature. FITC- and Cy5-conjugated goat anti-rabbit and anti-mouse secondary antibodies (Jackson ImmunoResearch) were diluted 1:1000 in PBT2. TOTO-3 iodide (Invitrogen) was diluted 1:2000. A 2-h incubation period in the secondary antibody mixture preceded three washes for 15 min each in PBS. The coverslipped specimens were analyzed by fluorescence or confocal microscopy (Zeiss Axioskop 2, Leica TCS SP2 or Zeiss LSM Pascal). The dynamin inhibitory peptide (DIP) and the membrane-permeant myristoylated DIP (Tocris Bioscience, Cologne, Germany) were dissolved in Me_2SO and added to the transfected cells at a concentration of 100 μM 16 h before fixation and immunostaining. The control cultures were treated with the appropriate amount of Me_2SO. For statistical analysis of our quantitative data, we performed unpaired Student's *t* tests using the Kaleidagraph software (Synergy, Reading, PA).

Electrophysiology—HEK293 cells were seeded 12–18 h after transfection onto poly-L-lysine-coated glass coverslips and incubated for 3 h before use. Whole cell currents utilizing ruptured patches were measured with an EPC-9 amplifier (HEKA Electronic, Lambrecht, Germany; sampling rate, 1 ms; 8-Pole Bessel filter 3kHz). Patch electrodes had a DC resistance of 2–4 MΩ when filled with intracellular solution. An Ag-AgCl wire was used as reference electrode. We used a ramp protocol, starting with a voltage step from 20 to −100 mV followed by a 400-ms linear ramp to +100 mV. This protocol was repeated every 5 s. The cell membrane capacitance values were used to calculate current densities. The standard extracellular solution contained 150 mM NaCl, 6 mM CsCl, 1 mM $MgCl_2$, 5 mM $CaCl_2$, 10 mM glucose, 10 mM HEPES, buffered at pH 7.4 (adjusted with NaOH). The pipette solution was composed of 20 mM CsCl, 100 mM Asp, 1 mM $MgCl_2$, 10 mM HEPES, 4 mM Na_2ATP, 10 mM BAPTA, 2.93 mM $CaCl_2$. The free Ca^{2+} concentration of this solution was 50 nM. The non-protein kinase C-activating phorbol ester, 4α-phorbol 12,13-dideconate (4α-PDD; Sigma), was applied at a 1 μM concentration from a 10 mM stock solution in ethanol.

Calcium Imaging—The cells were loaded with Fura-2 by adding 2 μM Fura-2 acetoxymethyl ester to the medium for 20 min at 37 °C. For imaging, the cells were perfused with an extracellular solution containing 150 mM NaCl, 6 mM CsCl, 1 mM $MgCl_2$, 1.5 mM $CaCl_2$, 10 mM HEPES, 10 mM glucose, buffered at pH 7.4, and 1 μM 4α-PDD was applied for activation. The intracellular $[Ca^{2+}]_i$ was measured with an imaging system consisting of a Polychrome IV monochromator (TILL Photonics, Martinsried, Germany) and a Roper Scientific charge-coupled device camera connected to an Axiovert 200M inverted microscope (Zeiss, Germany). Monochromator and camera were controlled with Metafluor software (version 6.3; Universal Imaging, Downingtown, PA). Fluorescence was measured during alternating excitation at 357 and 380 nm and corrected for the individual background fluorescence. The absolute Ca^{2+} concentration was obtained from the fluorescence ratios using the equation $[Ca^{2+}] = K_{eff}(R - R_0)/(R_1 - R)$, where K_{eff}, R_0, and R_1 are calibration constants. R_0 and R_1 were estimated by perfusing cells with Ca^{2+}-free solution and high Ca^{2+} containing solution, respectively. The effective binding constant, K_{eff}, was calculated by the equation $K_{eff} = K_d(R_1 + \alpha)/(R_0 + \alpha)$, where K_d is the dissociation constant of Fura-2, and α is the isocoefficient. K_d value was taken from Paltauf-Doburzynska and Graier (23). The isocoefficient α was obtained as described by Zhou and Neher (24).

RT-PCR—RT-PCR analysis of mouse tissues was performed using murine cDNA (mouse multiple tissue cDNA panel B; BD Biosciences) as template with the following oligonucleotides in standard PCRs: (i) PACSIN 3-forward, 5′-ttccgtaaagctcagaagccct-3′, and PACSIN 3-reverse, 5′-tgtcggtacaatgctggtcaga-3′; and (ii) TRPV4-forward, 5′-atcatcctcaccttcgtgctcctg-3′, and TRPV4-reverse, 5′-acaccggacaaatgcctaaatgta-3′. The amplification products were separated in a 1% agarose gel and documented using a digital camera system (Kodak).

RESULTS

Identification of PACSINs as TRPV4-binding Partners—We generated four different yeast two-hybrid bait vectors representing Gal4-binding domain fusions with the chicken TRPV4 amino terminus, each of the two intracellular loops and the carboxyl terminus. Only the amino-terminal bait yielded positive clones in yeast two-hybrid screening of a chicken inner ear cDNA library. We identified two groups of clones, all of which represented multiple in-frame isolates of different lengths of the chicken homologues for mammalian PACSINs 1 and 3 (18).

All Three PACSINs Bind to TRPV4—To confirm the yeast two-hybrid screening results, we sought to determine whether the mammalian isoforms of TRPV4 and PACSINs bind each other in biochemical assays. In co-immunoprecipitation experiments, we found that all three PACSINs were capable of precipitating co-expressed rat TRPV4 amino terminus (Fig. 1*B*).

Co-expression and immunoprecipitation of the full-length rat TRPV4 as well as murine TRPV4 with all three PACSINs confirmed this observation (Fig. 1, *C* and *D*). Neither mouse TRPV1 nor mouse TRPV2 were able to co-precipitate with any of the PACSIN family members, an indication that the binding between PACSINs and TRPV4 is specific (Fig. 1, *E* and *F*).

PACSIN 3, but Not PACSINs 1 and 2, Increases the Number of Cells Showing Predominant Plasma Membrane Association of TRPV4—Because the PACSINs have been implicated in endocytotic processes, we decided to investigate the subcellular distribution of TRPV4 in the presence of PACSINs. Therefore, we transfected HEK293, HeLa, and NIH 3T3 cells with expression vectors for each protein alone or in combinations. In all of the cell lines used for these studies, we obtained similar results: we noticed that the overall number of cells that displayed pronounced plasma membrane localization of TRPV4 was significantly increased from ~20–33% to 68–77%, depending on the cell type studied, when PACSIN 3 was co-transfected (77 ± 3.3%, mean ± S.E., $n = 3$, in HEK293 and 67.5 ± 2.9%, $n = 8$, in NIH 3T3 cells). Co-transfection with PACSINs 1 and 2 did not alter the number of cells with pronounced localization of TRPV4 in the plasma membrane, which was 20–33% (19.5 ± 1.8%, $n = 3$, for PACSIN 1 and 30.3 ± 0.3%, $n = 4$, for

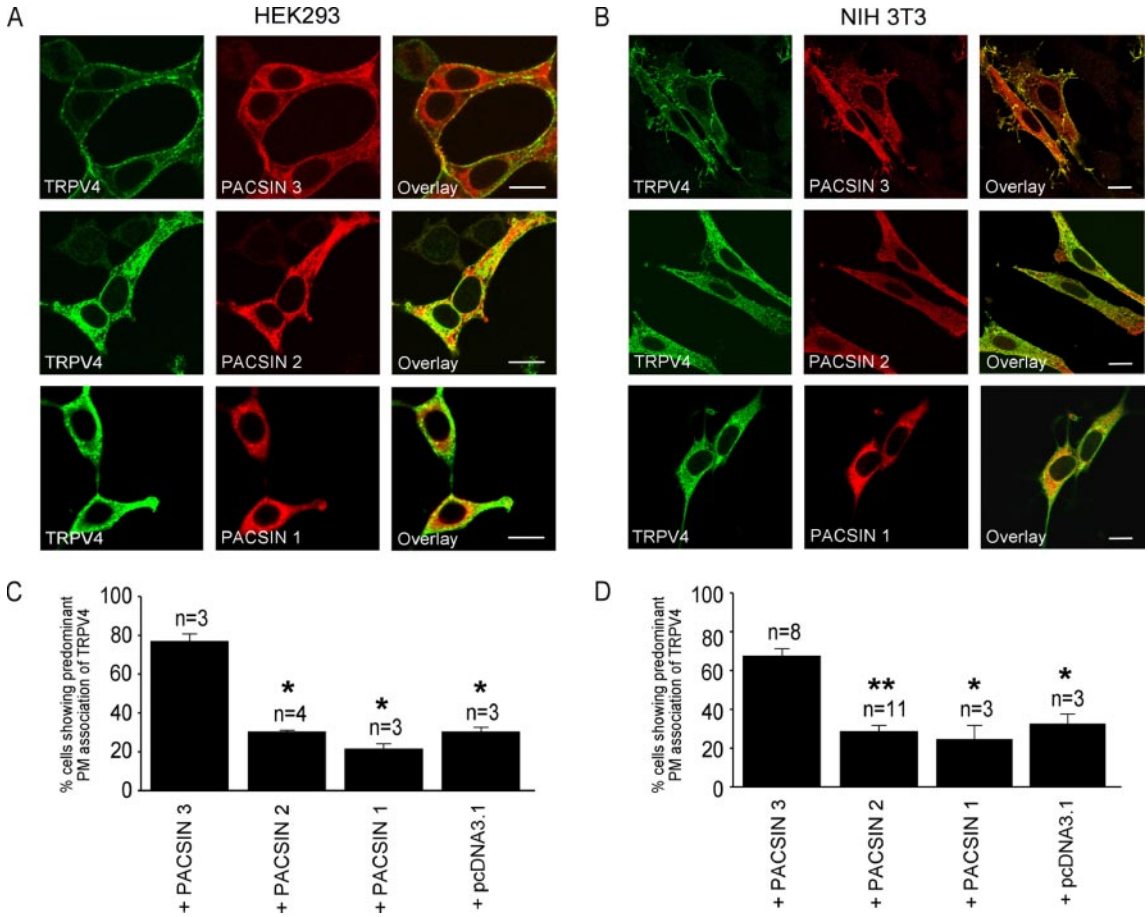

FIGURE 2. **Increase of TRPV4 plasma membrane association in presence of PACSIN 3.** *A* and *B*, comparison of the effect of co-expression of rat TRPV4 (FITC, shown in *green*) with PACSINs 1, 2 and 3 (Cy5, shown in *red*) in transfected HEK293 cells (*A*) and in NIH 3T3 cells (*B*). *Scale bar*, 16 μm. *C*, quantification of the number of HEK293 cells with clearly evident TRPV4 plasma membrane association as a fraction of the total cell number as a percentage. Shown are mean values ± S.E.; n = number of independent experiments with at least 20 randomly selected cells each. *, $p < 0.001$, Student's t test, unpaired comparison with PACSIN 3 co-transfection. *D*, same quantification as described in *C* with NIH 3T3 cells. Shown are the mean values ± S.E. *, $p < 0.001$; **, $p < 0.0001$, Student's t test, unpaired comparison with PACSIN 3 co-transfection. *PM*, plasma membrane.

PACSIN 2 in HEK293 and 24.2 ± 6.3%, $n = 3$, for PACSIN 1 and 28.6 ± 2.9%, $n = 11$, for PACSIN 2 in NIH 3T3 cells) (Fig. 2). Control vector co-expression also did not change the number of cells with pronounced TRPV4 plasma membrane localization (30.2 ± 1.6% in HEK293 and 32.7 ± 4.1% in NIH 3T3 cells).

Our co-immunoprecipitation results suggest that neither TRPV1 nor TRPV2 interact with any PACSIN protein. Co-expression of these TRPV family members with PACSINs 2 and 3 revealed no effect on their subcellular distribution (8.9 ± 3.9%, $n = 3$, for PACSIN 2 and 8.1 ± 1.0%, $n = 3$, for PACSIN 3 co-expressed with TRPV1; 74.5 ± 1.2%, $n = 3$, for PACSIN 2 and 70.6 ± 3.8%, $n = 4$, for PACSIN 3 co-expressed with TRPV2) (Fig. 3), suggesting that the effect of PACSIN 3 is specifically targeting TRPV4 and is not the result of a general inhibition of endocytosis.

PACSIN 3 Increases the Ratio of Plasma Membrane-associated TRPV4 versus Cytoplasmic TRPV4—To characterize the apparent effect of PACSIN 3 on the plasma membrane distribution of TRPV4 in more detail, we quantified the amount of plasma membrane-associated TRPV4 immunoreactivity as a fraction of the total amount of protein. Our experiments revealed an apparent increase of the plasma membrane association of TRPV4 to 86.9 ± 1.4% (mean ± S.E., $n = 3$) when we compared cells that co-expressed PACSIN 3 with cells co-transfected with empty vector (56.9 ± 5.1%, mean ± S.E., $n = 3$) or an expression vector for the PACSIN 3 SH3 domain mutant P415L (62.8 ± 0.7%, mean ± S.E., $n = 3$) (Fig. 4). This mutant has been reported to have lost its inhibitory effect on endocytosis (18), and it showed substantially reduced capacity to bind TRPV4 in co-immunoprecipitation assays (see below, Fig. 7*A*).

We next sought to determine whether the effect of PACSIN 3 on TRPV4 could lead to a measurable increase of TRPV4-mediated channel activity in response to the known TRPV4 agonist 4α-PDD (9). Analysis of the whole cell currents at a voltage potential of +100 mV revealed no statistically significant difference among HEK293 cells transfected with TRPV4, TRPV4/PACSIN 3, or TRPV4/PACSIN 3 mutant P415L. The basal current levels (in pA/pF; mean ± S.E.) for TRPV4, TRPV4/PACSIN 3, or TRPV4/PACSIN 3 mutant P415L were 108.0 ± 35.7, 62.9 ± 20.0, and 118.7 ± 35.7, respectively. In the presence of 1 μM 4α-PDD, a TRPV4 agonist, current levels (in pA/pF) increased to 511.0 ± 78.0, 543.7 ± 79.5, and 470 ± 67.7, respectively ($n = 5$–7). Similar results were observed in calcium imaging experiments for cells transfected with TRPV4 or co-transfected with PACSIN 3 or the PACSIN 3 mutant P415L. The absolute basal calcium levels for non-transfected, TRPV4, TRPV4/PACSIN 3, and TRPV4/PACSIN 3 mutant P415L cells were (mean ± S.E.): 80.37 ± 8.67 nM, 138.12 ± 58.3 nM, 118.71 ± 12.69 nM, and 173.58 ± 41.64 nM, respectively. Upon application of 1 μM 4α-PDD, the calcium levels rose to (mean ± S.E.): 86.87 ± 9.42 nM, 280.26 ± 70.8 nM, 356.95 ± 50.76 nM, and 339.15 ± 77.66 nM, respectively.

The Δ calcium concentration ($\Delta[Ca^{2+}] = [Ca^{2+}]_{max}$-$[Ca^{2+}]_{min}$) for nontransfected cells was 6.5 ± 4.21 nM. For the transfected cells we

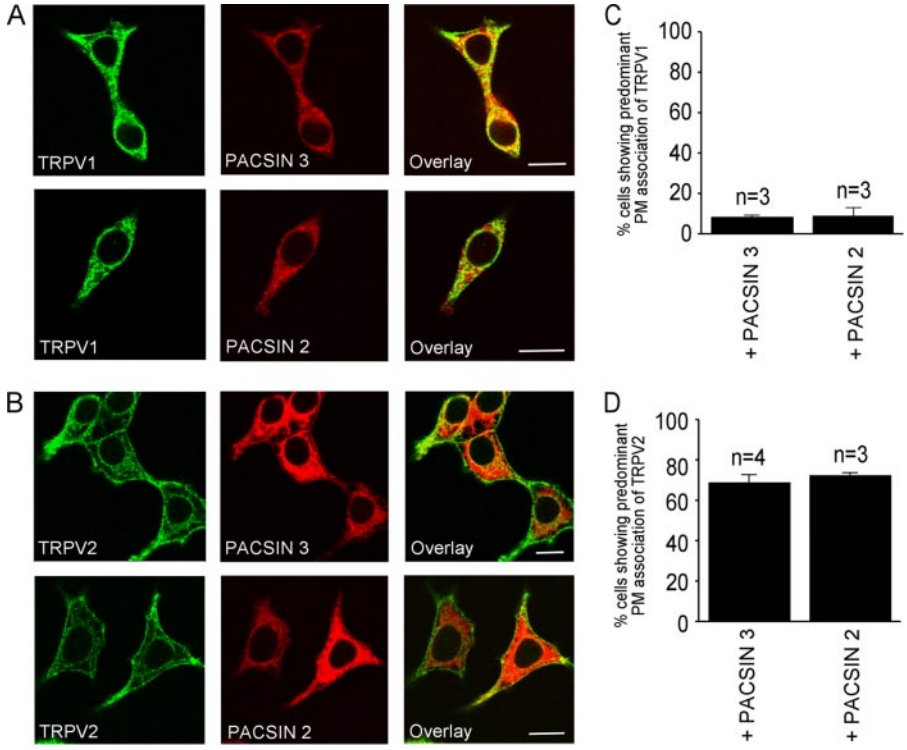

FIGURE 3. **PACSINs do not alter the subcellular distribution of TRPV1 and TRPV2.** Shown are immunofluorescence analyses of co-transfected HEK293 cells for TRPV1 and TRPV2 (FITC, shown in *green*) in the presence of either PACSIN 2 or PACSIN 3 (Cy5, shown in *red*). *A*, TRPV1 immunofluorescence appears punctate and associated with intracellular structures and faintly with the plasma membrane. This distribution does not change when either PACSIN protein is present; neither does it differ from HEK293 cells co-transfected with empty vector (not shown). *B*, TRPV2 immunofluorescence is largely associated with the plasma membrane, and this distribution is unaltered when either PACSIN protein is present; neither does it differ from HEK293 cells co-transfected with empty vector (not shown). The observed subcellular localization of TRPV1 and TRPV2 is in agreement with previous findings (44). *Scale bar*, 16 μm. *C*, quantification of the number of HEK293 cells with evident TRPV1 plasma membrane association as a fraction of the total cell number as a percentage in the presence of PACSIN 2 or PACSIN 3. *D*, quantification of the number of HEK293 cells with evident TRPV2 plasma membrane association as a fraction of the total cell number as a percentage in the presence of PACSIN 2 or PACSIN 3. Shown in *C* and *D* are the mean values ± S.E.; n = number of independent experiments with at least 20 randomly selected cells each. *PM*, plasma membrane.

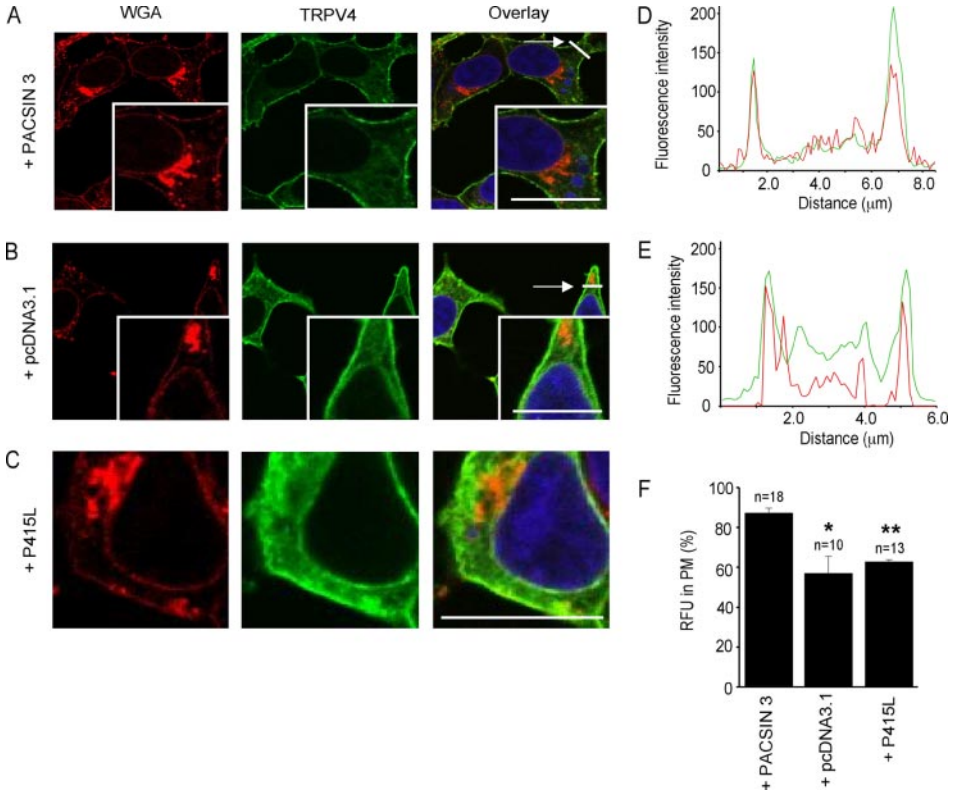

FIGURE 4. **Co-expression of PACSIN 3 diminishes intracellular TRPV4 and leads to apparent increase of TRPV4 membrane association.** *A–C*, immunolocalization of TRPV4 protein (FITC, shown in *green*) and co-labeling of membranes with Alexa Fluor 594-conjugated wheat germ agglutinin (*WGA*, shown in *red*) in HEK293 cells transfected with expression vectors for rat TRPV4 and PACSIN 3 (*A*), TRPV4 and empty vector (*B*), and TRPV4 and the P415L isoform of PACSIN 3 (*C*). *D*, fluorescence intensities of wheat germ agglutinin and TRPV4 immunoreactivities along the *line* marked by the *white arrow* in the overlay picture panel of *A*. *E*, same analysis as described in *D*, corresponding to the overlay panel of *B*. *F*, quantitative analysis of membrane-associated TRPV4 immunofluorescence as a fraction of the total TRPV4 immunofluorescence as a percentage determined from line scans of cells co-transfected with either PACSIN 3, empty vector, or the P415L mutant isoform of PACSIN 3. Shown are the mean values ± S.E. of line analyses derived from 18, 10, and 13 individual cells as indicated, respectively, randomly sampled from three independent experiments. The relative increase of TRPV4 membrane association is statistically significant (*, $p < 0.05$, when comparing PACSIN 3 with empty vector co-transfection and **, $p < 0.001$ when comparing PACSIN 3 with P415L co-transfection; Student's t test, unpaired). *Scale bar*, 16 μm.

obtained $\Delta[Ca^{2+}]$ of 141.4 ± 75.4 nM (TRPV4 alone), 238.2 ± 49.8 nM (TRPV4/PACSIN 3), and 165.6 ± 54.4 nM (TRPV4 and PACSIN 3 mutant P415L), respectively (n = 12–28). Measuring whole cell currents as well as the calcium imaging experiments revealed no significant variation among cells transfected with TRPV4 or co-transfected with PACSIN 3 or the PACSIN 3 mutant P415L.

The Dynamin Inhibitory Peptide Affects the Plasma Membrane Association of TRPV4—Changes in the ratio of plasma membrane-associated TRPV4 and cytoplasmic TRPV4 protein can be achieved by either modulating the transport of the ion channel to the plasma membrane or by affecting endocytotic processes. Because PACSIN 3 has been linked to inhibition of dynamin-mediated endocytosis (18), we decided to use

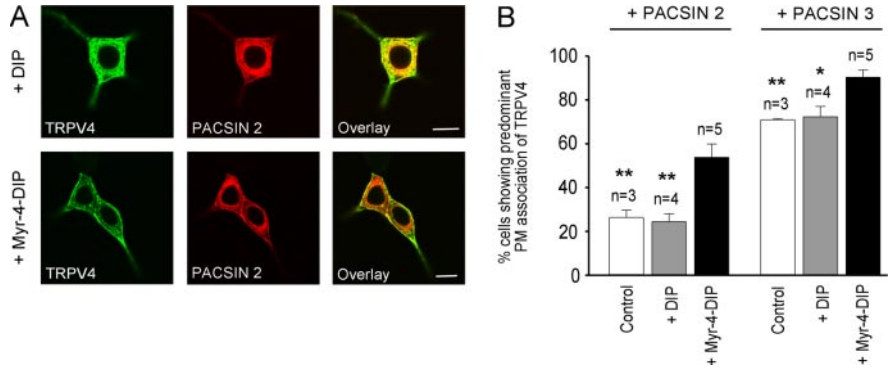

FIGURE 5. **Effects of PACSIN 3 and dynamin inhibitory peptide on TRPV4 membrane association.** *A*, immunolocalization of TRPV4 protein (FITC, shown in *green*) and PACSIN 2 (Cy5, shown in *red*) in transfected HEK293 cells treated with DIP and Myr-4-DIP. Shown are the predominant distributions of TRPV4 immunoreactivity, which are quantified in *B*. *B*, quantification of the number of HEK293 cells with clearly evident TRPV4 plasma membrane association as a fraction of the total cell number as a percentage. Shown are the mean values ± S.E.; n = number of independent experiments with at least 20 randomly selected cells each. *, $p < 0.05$; **, $p < 0.01$, Student's t test, unpaired. *PM*, plasma membrane.

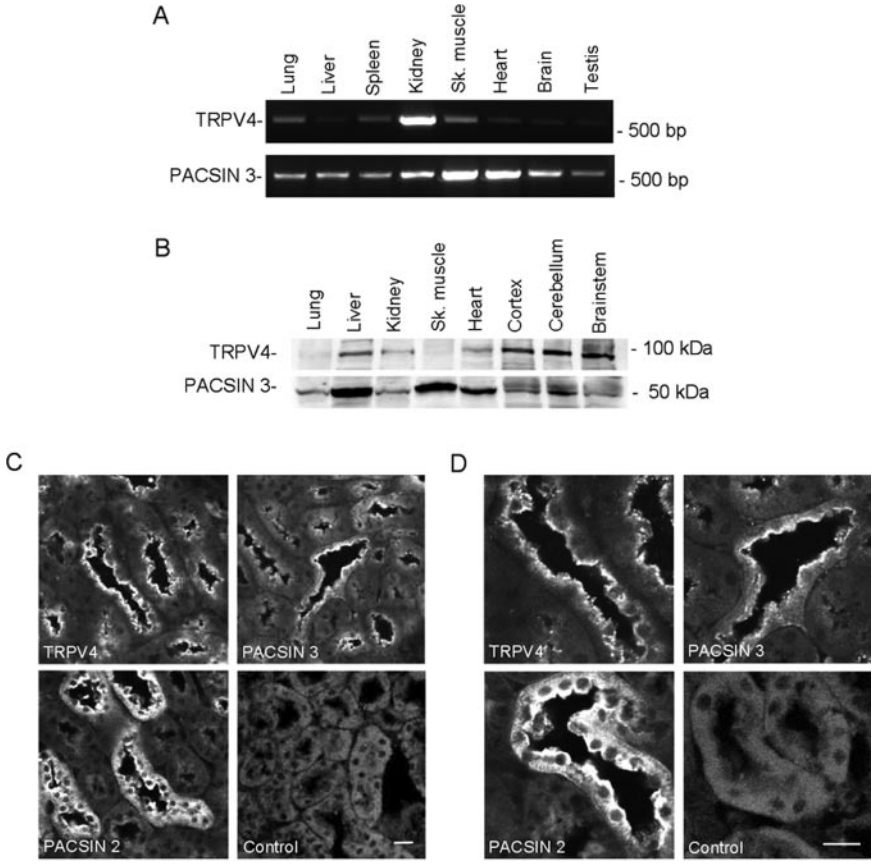

FIGURE 6. **Overlapping expression of TRPV4 and PACSIN 3.** *A* and *B*, RT-PCR (*A*) and Western blot (*B*) analyses of the expression of TRPV4 (expected RT-PCR fragment size, 586 bp) and PACSIN 3 (expected RT-PCR fragment size, 588 bp) in various murine organs. *C* and *D*, immunolocalization of TRPV4, PACSIN 3, and PACSIN 2 protein to renal tubule cells. Note that TRPV4 and PACSIN 3 are located in the luminal plasma membrane of the tubule cells, whereas strongly expressed PACSIN 2 appears to be cytoplasmic. *Control*, omission of the primary antibody. The secondary antibody was Cy5-conjugated antibody to rabbit IgG. *Scale bars*, 20 μm in *C* and *D*.

a previously described dynamin inhibitory peptide (25). Dynamin inhibitory peptide specifically competes with the dynamin-binding site of amphiphysin (25), thereby preventing the initial steps of dynamin-mediated endocytotic processes. If this process regulates TRPV4 plasma membrane association, one would expect an effect in cells treated with the dynamin inhibitory peptide. Indeed, the membrane-permeable form of the dynamin inhibitory peptide (Myr-4-DIP), but not the impermeable version (DIP), significantly increased the fraction of cells with predominant TRPV4 plasma membrane expression (Fig. 5). In the presence of PACSIN 2, here used as a control that apparently does not affect the distribution of TRPV4 (Fig. 2), the fraction of cells with predominant plasma membrane expression of TRPV4 was 53.6 ± 6.2% (mean ± S.E., $n = 5$) in cells treated with Myr-4-DIP *versus* 24.3 ± 3.5% (mean ± S.E., $n = 4$) in cells treated with DIP. When we added Myr-4-DIP to cells co-expressing PACSIN 3 and TRPV4, we observed a further significant increase of the cell population with predominant TRPV4 plasma membrane expression compared with the impermeable version of the peptide (90.4 ± 3.1%, $n = 5$ *versus* 72.3 ± 4.5%, $n = 4$, respectively). Myr-4-DIP alone in the absence of PACSIN 2 or PACSIN 3 showed an increase that was less effective than with co-expression of PACSIN 2 or 3 (data not shown). Our results suggest that the mechanism of the interaction between PACSIN 3 and TRPV4 is similar to the effect of the dynamin inhibitory peptide, which supports the conclusion that PACSIN 3 inhibits TRPV4 endocytosis.

TRPV4 and PACSIN 3 Are Widely Expressed and Co-localize in Kidney Tubule Membranes—The effects of PACSIN 3 on TRPV4 are only biologically relevant when the expression of both proteins overlaps *in vivo*. Comparison of the expression patterns of both proteins by RT-PCR and by Western blot analysis revealed widespread expression of TRPV4 and PACSIN3 in many different organs (Fig. 6, *A* and *B*). To demonstrate co-localization of the two proteins, we decided to focus on the kidney, and we found TRPV4 and PACSIN 3 immunoreactivity associated with the luminal membranes of kidney tubules (Fig. 6, *C* and *D*). This observation is supported by previous studies that describe

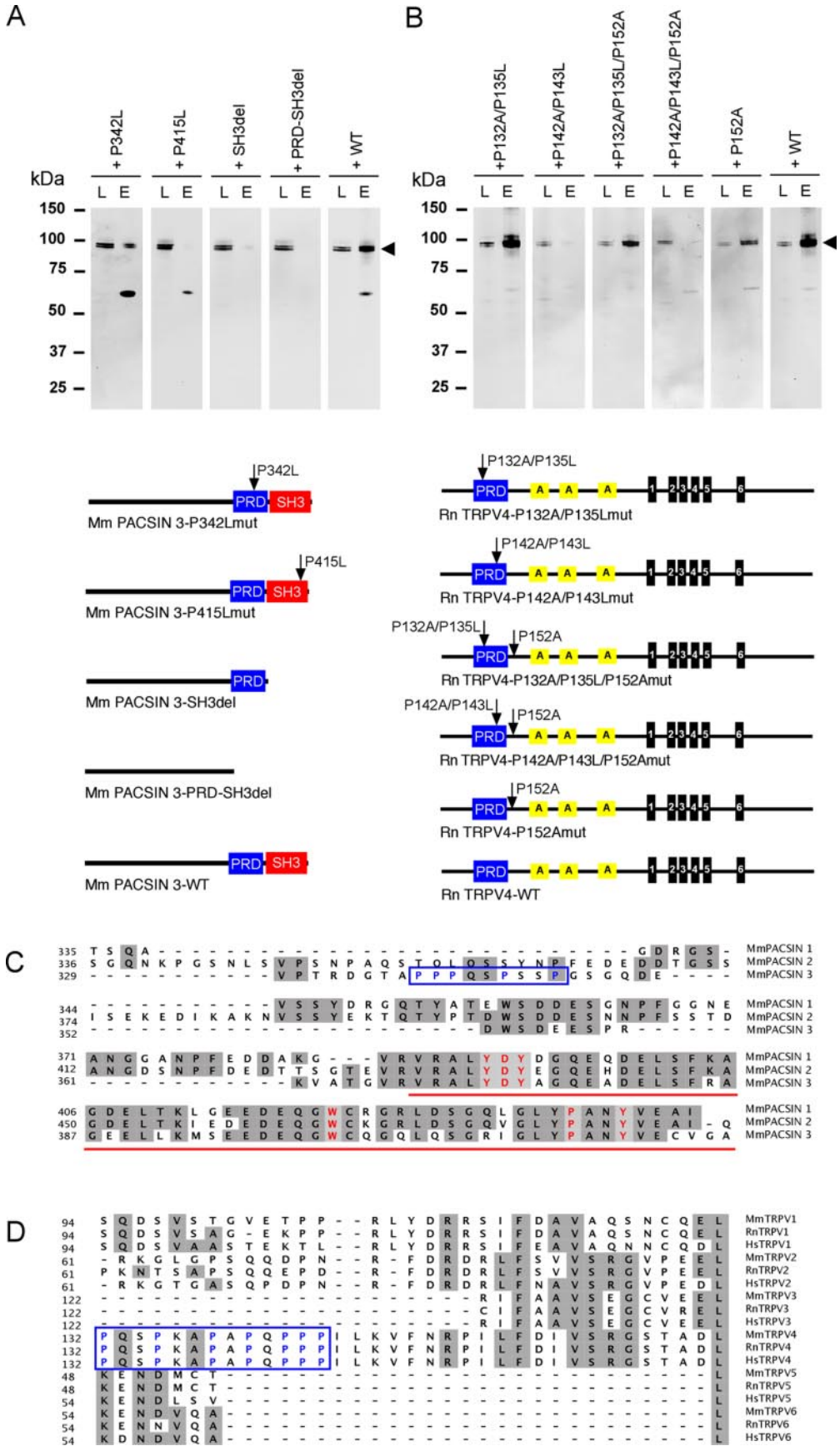

FIGURE 7. **Mapping of the TRPV4-PACSIN 3 interaction sites.** *A*, Western blot analysis showing co-precipitation of rat TRPV4 with Myc-tagged PACSIN 3 deletion and point mutants. *B*, Western blot analysis showing co-precipitation of rat TRPV4 point mutants with Myc-tagged PACSIN 3. The occasionally occurring ~60-kDa band noticeable in some of the lanes was observable in some but not all experiments. *L*, lysate; *E*, elution from immunoprecipitate. Immunoprecipitation was done with immobilized 9E10 antibody, and TRPV4 was

expression of PACSIN 3 in the kidney (18, 26). TRPV4 immunoreactivity in the kidney has previously been reported in the luminal membrane (27) as well as in the basolateral plasma membrane (28). PACSIN 2 was also expressed in renal tubule cells, but its subcellular location was not limited to the luminal plasma membrane. PACSIN 1 was not detectable in kidney.

The Carboxyl-terminal SH3 Domain of PACSIN 3 Binds to an Amino-terminal PRD of TRPV4—All PACSINs contain a carboxyl-terminal SH3 domain (18). We generated point mutations and deletion mutants in the carboxyl terminus of PACSIN 3 to test which parts of the protein are essential for binding TRPV4 (Fig. 7, *A* and *C*). In co-immunoprecipitation experiments, we found that complete deletion of the SH3 domain abolished TRPV4 binding, and introduction of a point mutation at position 415 (P415L) greatly diminished TRPV4 binding. The P415L mutation has been described before as deficient in binding PRD containing proteins such as dynamin (18). Our results suggest that the SH3 domain of PACSIN 3 is essential for TRPV4 binding.

Because SH3 domains have been reported to bind PRD motifs (29, 30), we turned our attention to the PRD motif located in the amino terminus of TRPV4 (Fig. 7*D*). Mutating proline residues at positions 142 and 143 to alanine and leucine, respectively, resulted in substantial reduction or abolishment of PACSIN 3 binding (Fig. 7*B*). Likewise, PACSINs 1 and 2 were not able to co-immunoprecipitate this mutant (data not shown). These results suggest that the two amino acids of the triple-proline motif in the amino-terminal PRD of TRPV4 are essential for the binding of PACSINs.

DISCUSSION

The main conclusion of our study is that PACSIN 3, a protein that has been implicated to block dynamin-mediated endocytosis, functionally interacts with the cation channel TRPV4. TRPV4 is also capable of biochemically interacting with PACSINs 1 and 2, but co-expression of these two PACSINs did not affect the plasma membrane association of TRPV4. The expression of PACSIN 1 is restricted to the central nervous system, whereas PACSINs 2 and 3 are expressed in many other non-neural organs and tissues (18, 21, 31). In the kidney, we found that only PACSIN 3 and TRPV4 occur at common subcellular locations, suggesting that these two proteins are potentially able to engage in a physiologically relevant interaction *in vivo*.

There is a discrepancy in the literature describing TRPV4 localization in kidney tubule cells as being associated either with the luminal plasma membrane (27) or with the basolateral membrane (28). The former study used a polyclonal antibody raised to an 11-amino acid-long carboxyl-terminal TRPV4 peptide, whereas the latter study utilized an anti-peptide antibody raised to a longer version of the peptide with 8 additional amino acids (32). The specificity of the affinity-purified antibody to the first 233 amino-terminal amino acids of rat TRPV4 used in our study was confirmed by blocking of the TRPV4 Western blot signal with antigen preincubation. Further confirmation and characterization of the antibody in earlier reports show lack of a specific TRPV4 band on Western blots and lack of signal in immunocytochemistry of primary cells done with tissues taken from TRPV4 knock-out mice (11, 12). We are thus confident that the control experiments performed herein and by other groups who used our antibody thoroughly demonstrate its specificity.

The binding of PACSIN proteins to TRPV4 is specific because we could not detect binding of any PACSINs to the related TRPV1 and TRPV2 ion channels. We have identified a triple-proline motif within the PRD in the amino terminus of TRPV4 as the binding site for PACSINs 1, 2, and 3. Sequence comparisons reveal that this motif does not occur in any other TRPV protein (Fig. 7*D*), further substantiating the specificity of the TRPV4 and PACSIN 3 interaction via binding of the SH3 domain (Fig. 7, *A* and *C*).

When we co-transfected TRPV4 with PACSIN 3, we made two principal observations. First, the ratio of TRPV4 associated with the plasma membrane when compared with intracellular TRPV4 increased significantly, and second, the number of cells with predominantly plasma membrane-associated TRPV4 increased from ~30% of the total cell number to 68–77%. This effect was specific because it was not detectable when we co-transfected PACSIN 1, PACSIN 2, or P415L, a mutant isoform of PACSIN 3 that shows greatly reduced binding to TRPV4.

The most plausible explanation for the apparent PACSIN 3-dependent increase of the quantity of TRPV4 immunoreactivity in the plasma membrane is that PACSIN 3 blocks endocytosis of the ion channel. Despite their ability to bind to TRPV4, PACSINs 1 and 2 do not have a detectable effect. Our biochemical studies revealed no binding of PACSIN proteins to other TRPV channels, and we confirmed that neither PACSIN 2 nor PACSIN 3 altered the subcellular distribution of TRPV1 or TRPV2, suggesting that the effect of PACSIN 3 specifically targeted TRPV4. Inhibition of dynamin-mediated endocytosis affects TRPV4 in a fashion similar to that of PACSIN 3 co-expression, indicating that endocytosis of TRPV4 is a probable target of PACSIN 3. This interpretation of our data is based on the assumption that neither the effect of the dynamin-inhibiting peptide nor the effect of PACSIN 3 co-expression is complete.

The PACSINs contain a well characterized carboxyl-terminal SH3 domain, a *Schizosaccharomyces pombe* CDC15p amino-terminal domain (CDC15-NT) and a proposed coiled-coil forming region (18, 34). PACSINs 1 and 2, but not PACSIN 3, have NPF (asparagine, proline, and phenylalanine) motifs located between the CDC15-NT and SH3 domain (18, 34). In contrast, only PACSIN 3 has a PRD motif between the CDC15-NT and SH3 domain (Fig. 7*C*). PRD motifs display affinity for specific SH3 domains in other proteins (27).

We propose that the PRD in PACSIN 3 has a modulating function in dynamin-mediated endocytotic processes. It is known that the SH3 domain of all PACSINs can interfere with dynamin function by interacting with its PRD (18). In parallel, the PRD of PACSIN 3 may additionally displace dynamin interactions with other SH3 domain proteins that are part of the endocytotic machinery such as amphiphysin, Grb2, or endophilin (33–35). Consequently, we hypothesize that the lack of the PRD in PACSINs 1 and 2 may explain their functional differences to PACSIN 3. This second function of PACSIN 3 would explain why PACSIN 2 in combination with Myr-4-DIP is more effective than Myr-4-DIP alone and about as effective as PACSIN 3 alone.

The blockade of TRPV4 endocytosis leads to accumulation of the channel protein in or near the plasma membrane and to a noticeable decrease of intracellular TRPV4 immunoreactivity. With the resolution of the confocal microscope, however, it is not clear whether TRPV4 accumulates in or in close vicinity to the plasma membrane.

We hypothesized that increased TRPV4 channel numbers in the plasma membrane will only be revealed by electrophysiological or cal-

detected with polyclonal antibody. *C*, protein sequence alignment of the carboxyl termini of murine PACSINs 1–3. Conserved amino acid residues are highlighted by *gray shading*. The SH3 domain is underlined with a *red bar*, and the SH3 core residues are labeled in *red*. Conserved consensus hydrophobic residues of the SH3 domain involved in binding proline residues are shown in *red*. The PRD, which is unique to PACSIN 3, is framed with a *blue box*. *D*, sequence comparison of the amino termini of all six TRPV channel subfamily members in three mammalian species. *Mm*, *Mus musculus*; *Rn*, *Rattus norvegicus*; *Hs*, *Homo sapiens*. The TRPV4-specific PRD, including the triple-proline (*PPP*) motif, which we propose as the binding site for the SH3 domain of PACSIN 3, is decorated with a *blue box*.

cium imaging techniques. We did not, however, see any appreciable effects upon co-expression of PACSIN 3 and TRPV4 in HEK293 cells. One possible interpretation of these results is that PACSIN 3-affected channels may only be located in close proximity, but not necessarily in the plasma membrane. Alternatively, PACSIN 3-bound TRPV4 channels might be nonfunctional or unresponsive to 4α-PDD as a direct consequence of PACSIN 3 binding, which thus raises the question of whether PACSIN 3 could function as a direct regulator of TRPV4 activity. Our results do not exclude a functional effect of PACSIN 3 on the channel features of TRPV4; they reveal, however, that future investigation of their interaction may require a much more detailed analysis. Ultimately, it might be necessary to compare single channel features of PACSIN 3-bound TRPV4 *versus* unbound TRPV4.

The plasma membrane distribution of ion channels is tightly regulated, and these proteins undergo rapid endocytosis for either subsequent recycling or degradation (36). Thus, discrete membrane trafficking proteins regulate the turnover of ion channels from the endoplasmic reticulum to the *trans*-Golgi network, where they are subsequently directed in a compartmentalized manner to the plasma membrane to take on their various critical roles in ion homeostasis and signal transduction mechanisms (37). Disturbances in subcellular trafficking of ion channels have been linked with human diseases like cystic fibrosis, Mucolipidosis type IV (TRPML1), and polycystic kidney disease (TRPP2) (37–42). Recently, MAP7 (microfilament-associated protein 7) has also been implicated to increase the membrane expression of TRPV4 (27). The interaction of MAP7 with TRPV4 appears to occur at the carboxyl terminus of TRPV4 between amino acids 789 and 809, and in contrast to the interaction of PACSIN 3 with TRPV4, it does not appear to involve regulation of endocytosis. It will be interesting to test whether PACSIN 3-mediated and MAP7-mediated regulation of the plasma membrane association of TRPV4 act in cooperation in cell types that express all three proteins.

The widespread cellular distribution of TRPV4 and PACSIN 3 implies that each protein has multiple functions, some of which may be completely independent of each other. We focused our analysis of native cellular localization studies of these proteins on mouse kidney tissue because both proteins had previously been reported to be expressed in this organ, and it has been postulated that association with the luminal plasma membrane of an osmosensitive cation channel in the kidney is of relevance because its function may involve feedback regulation of ion homeostasis (1, 2, 18, 43). If the physiological function of TRPV4 in this organ requires strict regulation of membrane recycling, degradation, and intracellular membrane shuttling, then PACSIN 3, perhaps in concert with MAP7, is a plausible candidate to be involved in this complex mechanism.

Acknowledgments—We thank S. Mann and B. Merkl for expert technical help and the members of our laboratory group for comments on the manuscript. We thank Dr. M. Caterina (The Johns Hopkins University School of Medicine) for the murine TRPV1 cDNA.

REFERENCES

1. Strotmann, R., Harteneck, C., Nunnenmacher, K., Schultz, G., and Plant, T. D. (2000) *Nat. Cell Biol.* **2,** 695–702
2. Liedtke, W., Choe, Y., Marti-Renom, M. A., Bell, A. M., Denis, C. S., Sali, A., Hudspeth, A. J., Friedman, J. M., and Heller, S. (2000) *Cell* **103,** 525–535
3. Wissenbach, U., Bodding, M., Freichel, M., and Flockerzi, V. (2000) *FEBS Lett.* **485,** 127–134
4. Delany, N. S., Hurle, M., Facer, P., Alnadaf, T., Plumpton, C., Kinghorn, I., See, C. G., Costigan, M., Anand, P., Woolf, C. J., Crowther, D., Sanseau, P., and Tate, S. N. (2001) *Physiol. Genomics* **4,** 165–174
5. Watanabe, H., Vriens, J., Prenen, J., Droogmans, G., Voets, T., and Nilius, B. (2003) *Nature* **424,** 434–438
6. Nilius, B., Watanabe, H., and Vriens, J. (2003) *Pflugers Arch. Eur. J. Physiol.* **446,** 298–303
7. Guler, A. D., Lee, H., Iida, T., Shimizu, I., Tominaga, M., and Caterina, M. (2002) *J. Neurosci.* **22,** 6408–6414
8. Watanabe, H., Vriens, J., Suh, S. H., Benham, C. D., Droogmans, G., and Nilius, B. (2002) *J. Biol. Chem.* **277,** 47044–47051
9. Watanabe, H., Davis, J. B., Smart, D., Jerman, J. C., Smith, G. D., Hayes, P., Vriens, J., Cairns, W., Wissenbach, U., Prenen, J., Flockerzi, V., Droogmans, G., Benham, C. D., and Nilius, B. (2002) *J. Biol. Chem.* **277,** 13569–13577
10. Vriens, J., Watanabe, H., Janssens, A., Droogmans, G., Voets, T., and Nilius, B. (2004) *Proc. Natl. Acad. Sci. U. S. A.* **101,** 396–401
11. Liedtke, W., and Friedman, J. M. (2003) *Proc. Natl. Acad. Sci. U. S. A.* **100,** 13698–13703
12. Chung, M. K., Lee, H., Mizuno, A., Suzuki, M., and Caterina, M. J. (2004) *J. Biol. Chem.* **279,** 21569–21575
13. Gopinath, P., Wan, E., Holdcroft, A., Facer, P., Davis, J. B., Smith, G. D., Bountra, C., and Anand, P. (2005) *BMC Womens Health* **5,** 2
14. Alessandri-Haber, N., Yeh, J. J., Boyd, A. E., Parada, C. A., Chen, X., Reichling, D. B., and Levine, J. D. (2003) *Neuron* **39,** 497–511
15. Alessandri-Haber, N., Dina, O. A., Yeh, J. J., Parada, C. A., Reichling, D. B., and Levine, J. D. (2004) *J. Neurosci.* **24,** 4444–4452
16. Suzuki, M., Watanabe, Y., Oyama, Y., Mizuno, A., Kusano, E., Hirao, A., and Ookawara, S. (2003) *Neurosci. Lett.* **353,** 189–192
17. Suzuki, M., Mizuno, A., Kodaira, K., and Imai, M. (2003) *J. Biol. Chem.* **278,** 22664–22668
18. Modregger, J., Ritter, B., Witter, B., Paulsson, M., and Plomann, M. (2000) *J. Cell Sci.* **113,** 4511–4521
19. Heller, S., Sheane, C. A., Javed, Z., and Hudspeth, A. J. (1998) *Proc. Natl. Acad. Sci. U. S. A.* **95,** 11400–11405
20. Gietz, R. D., and Woods, R. A. (2002) *Methods Enzymol.* **350,** 87–96
21. Plomann, M., Lange, R., Vopper, G., Cremer, H., Heinlein, U. A., Scheff, S., Baldwin, S. A., Leitges, M., Cramer, M., Paulsson, M., and Barthels, D. (1998) *Eur. J. Biochem.* **256,** 201–211
22. Qualmann, B., and Kelly, R. B. (2000) *J. Cell Biol.* **148,** 1047–1062
23. Paltauf-Doburzynska, J., and Graier, W. F. (1997) *Cell Calcium* **21,** 43–51
24. Zhou, Z., and Neher, E. (1993) *Pflugers Arch.* **425,** 511–517
25. Nong, Y., Huang, Y. Q., Ju, W., Kalia, L. V., Ahmadian, G., Wang, Y. T., and Salter, M. W. (2003) *Nature* **422,** 302–307
26. Sumoy, L., Pluvinet, R., Andreu, N., Estivill, X., and Escarceller, M. (2001) *Gene (Amst.)* **262,** 199–205
27. Suzuki, M., Hirao, A., and Mizuno, A. (2003) *J. Biol. Chem.* **278,** 51448–51453
28. Tian, W., Salanova, M., Xu, H., Lindsley, J. N., Oyama, T. T., Anderson, S., Bachmann, S., and Cohen, D. M. (2004) *Am. J. Physiol.* **287,** F17–F24
29. Owen, D. J., Wigge, P., Vallis, Y., Moore, J. D., Evans, P. R., and McMahon, H. T. (1998) *EMBO J.* **17,** 5273–5285
30. Mott, H. R., Nietlispach, D., Evetts, K. A., and Owen, D. (2005) *Biochemistry* **44,** 10977–10983
31. Qualmann, B., Roos, J., DiGregorio, P. J., and Kelly, R. B. (1999) *Mol. Biol. Cell* **10,** 501–513
32. Xu, H., Zhao, H., Tian, W., Yoshida, K., Roullet, J. B., and Cohen, D. M. (2003) *J. Biol. Chem.* **278,** 11520–11527
33. Miki, H., Miura, K., Matuoka, K., Nakata, T., Hirokawa, N., Orita, S., Kaibuchi, K., Takai, Y., and Takenawa, T. (1994) *J. Biol. Chem.* **269,** 5489–5492
34. Seedorf, K., Kostka, G., Lammers, R., Bashkin, P., Daly, R., Burgess, W. H., van der Bliek, A. M., Schlessinger, J., and Ullrich, A. (1994) *J. Biol. Chem.* **269,** 16009–16014
35. Simpson, F., Hussain, N. K., Qualmann, B., Kelly, R. B., Kay, B. K., McPherson, P. S., and Schmid, S. L. (1999) *Nat. Cell Biol.* **1,** 119–124
36. Bezzerides, V. J., Ramsey, I. S., Kotecha, S., Greka, A., and Clapham, D. E. (2004) *Nat. Cell Biol.* **6,** 709–720
37. Kottgen, M., Benzing, T., Simmen, T., Tauber, R., Buchholz, B., Feliciangeli, S., Huber, T. B., Schermer, B., Kramer-Zucker, A., Hopker, K., Simmen, K. C., Tschucke, C. C., Sandford, R., Kim, E., Thomas, G., and Walz, G. (2005) *EMBO J.* **24,** 705–716
38. Cheng, S. H., Gregory, R. J., Marshall, J., Paul, S., Souza, D. W., White, G. A., O'Riordan, C. R., and Smith, A. E. (1990) *Cell* **63,** 827–834
39. Koulen, P., Cai, Y., Geng, L., Maeda, Y., Nishimura, S., Witzgall, R., Ehrlich, B. E., and Somlo, S. (2002) *Nat. Cell Biol.* **4,** 191–197
40. Sun, M., Goldin, E., Stahl, S., Falardeau, J. L., Kennedy, J. C., Acierno, J. S., Jr., Bove, C., Kaneski, C. R., Nagle, J., Bromley, M. C., Colman, M., Schiffmann, R., and Slaugenhaupt, S. A. (2000) *Hum. Mol. Genet* **9,** 2471–2478
41. Jentsch, T. J., Hubner, C. A., and Fuhrmann, J. C. (2004) *Nat. Cell Biol.* **6,** 1039–1047
42. Hanaoka, K., Qian, F., Boletta, A., Bhunia, A. K., Piontek, K., Tsiokas, L., Sukhatme, V. P., Guggino, W. B., and Germino, G. G. (2000) *Nature* **408,** 990–994
43. Kessels, M. M., and Qualmann, B. (2004) *J. Cell Sci.* **117,** 3077–3086
44. Hellwig, N., Albrecht, N., Harteneck, C., Schultz, G., and Schaefer, M. (2005) *J. Cell Sci.* **118,** 917–928